Applied Biochemistry and Biotechnology (2021) 193:1482–1495
https://doi.org/10.1007/s12010-021-03487-y

ORIGINAL ARTICLE

Biochemical Properties of a Novel D-Mannose Isomerase from *Pseudomonas syringae* for D-Mannose Production

Xiaohan Hua[1] · Yanxiao Li[2] · Zhengqiang Jiang[1] · Junwen Ma[2] · Haijie Liu[1] · Qiaojuan Yan[2]

Received: 1 August 2020 / Accepted: 7 January 2021 /
Published online: 23 January 2021

Abstract

D-Mannose isomerase can reversibly catalyze D-fructose to D-mannose which has various beneficial effects. A novel D-mannose isomerase gene (*PsMIaseA*) from *Pseudomonas syringae* was cloned and expressed in *Escherichia coli*. The recombinant D-mannose isomerase (*Ps*MIaseA) showed the highest amino acid sequence homogeneity of 50% with ManI from *Thermobifda fusca*. *Ps*MIaseA was purified through Ni-NTA chromatography, and its specific activity was 818.6 U mg^{-1}. The optimal pH and temperature of *Ps*MIaseA were pH 7.5 and 45 °C, respectively. The enzyme was stable within a wide pH range from 5.0 to 10.0. It could efficiently convert D-fructose to D-mannose without any metal ions. When *Ps*MIaseA was incubated with 600 g/L D-fructose for 6 h, the space-time yield of D-mannose reached 27.2 g L^{-1} h^{-1} with a maximum conversion ratio of 27%. Therefore, the D-mannose isomerase may be suitable for green production of D-mannose.

Keywords Mannose · Mannose isomerase · Characterization · *Pseudomonas syringae* · Mannose production

Xiaohan Hua and Yanxiao Li contributed equally to this work.

✉ Qiaojuan Yan
yanqj@cau.edu.cn

[1] Key Laboratory of Food Bioengineering (China National Light Industry), College of Food Science and Nutritional Engineering, China Agricultural University, No.17 Qinghua Donglu, Haidian District, Beijing 100083, China

[2] Beijing Advanced Innovation Center for Food Nutrition and Human Health, College of Engineering, China Agricultural University, No.17 Qinghua Donglu, Haidian District, Beijing 100083, China

Introduction

High-sugar diets have led to an increasing incidence of obesity and diabetes worldwide. Thus, low-sugar diets have attracted widespread attention from both researchers and consumers [1]. To reduce the amount of sugar in food, some monosaccharides with low calorie and multiple functions have been used as sugar substitutes. Among monosaccharides, D-mannose is the aldose isomer of D-fructose as well as the C-2 epimer of D-glucose. Its sweetness is 60% of sucrose, and its caloric value is 3.75 kcal g^{-1} [2]. Mannose has attracted great attention owing to its numerous health benefits, such as regulating immunity and metabolism [3], preventing urinary tract infections [4], promoting the proliferation of intestinal probiotics [5], and retarding tumor growth [6]. Moreover, it has been used as an additive in feed to prevent *Salmonella contamination* [7] as well as a precursor in medicine to produce anti-tumor agents, polyol, and vitamins [8–10]. Efficient and green production of mannose has become a new development direction for food and bioproduct industries.

In nature, mannose is a common component of mannan and a sugar chain of glycoprotein [11]. Small amount of mannose in free form has been found in some plants and animals. It is difficult to extract mannose directly from plants, such as fruits [12] and herbs [13]. Chemical conversion of glucose is now the main method for mannose production [14]. Normally, this process is carried out under high temperature condition with a large amount of acid and molybdate. It can cause high energy consumption, byproduct formation, complex downstream purification, and environmental pollution. By contrast, enzyme method can produce mannose at a mild condition with eco-friendliness and high efficiency, and has attracted increasing attention [15]. There are four main types of enzymes which produce mannose: D-mannose isomerase (EC 5.3.1.7), D-lyxose isomerase (EC 5.3.1.15), D-mannose 2-epimerase (EC 5.1.3.-), and cellobiose 2-epimerase (EC 5.1.3.11) [16]. The former two enzymes can catalyze the isomerization between mannose and fructose, whereas the latter two mainly catalyze the C-2 epimerization between mannose and glucose. However, neither lyxose isomerase nor cellobiose 2-epimerase is suitable for the production of mannose due to their metal ion dependence and low substrate specificity [17, 18]. Mannose isomerase can specifically isomerize fructose to mannose without metal ion dependence [19].

Mannose isomerase was first found in *Pseudomonas saccharophila* in 1956 [20]. Thereafter, some mannose isomerases have been identified and characterized [21, 22]. Only a few of them have been heterologously expressed in *E. coli*, such as those from *Salmonella enterica* [23] and *Thermobifida fusca* [24]. To improve the expression level, a mannose isomerase (MIase) from *E. coli* BL21 has been expressed in *Bacillus subtilis* WB800 with extracellular activity of 51.2 U mL^{-1} [25]. Normally, mannose isomerases show the highest catalytic activity in the neutral-to-alkaline range and reversibly convert fructose to mannose with an equilibrium ratio ranging from 20 to 35% [26, 27]. It is gradually realized that mannose isomerase is a suitable enzyme for green production of mannose.

Pseudomonas syringae can produce a variety of enzymes related to sugar metabolism [28]. Herein, a mannose isomerase gene from *P. syringae* was cloned and expressed in *E. coli*. Biochemical properties of the recombinant enzyme were measured, and the subsequent evaluation of its application in mannose production was conducted. It is the first report on mannose isomerase from *P. syringae*.

Materials and Methods

Chemicals and Reagents

E. coli BL21 (DE3), serving as the heterologous expression host, was acquired from Invitrogen (Carlsbad, CA). Plasmid pET28a (+) as an expression vector was purchased from Novagen (Madison, WI). Mannose and fructose were provided by BioDee (Beijing, China). The fructose assay kit was obtained from Nanjing Jiancheng Bioengineering Institute (Nanjing, China).

Cloning and Expression of the Mannose Isomerase Gene

Based on the genomic DNA of *P. syringae* in the GenBank database, the mannose isomerase gene (GenBank accession number WP_007249212.1), designated as *PsMIaseA*, was amplified by PCR with primers *PsMIaseA*F (GAGAGATCCATATGGACAACAACAACCACACCTTCA) and *PsMIaseA*R (GATCACTCGCTCGAGTGAAGGTGTGGTTGTTGTTGTCCAT). The PCR products were digested with *Nde*I and *Xho*I, and inserted into pET28a (+) vector (Novagen, USA). For heterologous expression, the consequent recombinant plasmids (pET28a-*PsMIaseA*) were introduced into *E. coli* BL21 competent cells.

The recombinant cells carrying the pET28a-*PsMIaseA* plasmid were cultured into the LB medium containing 50 μg mL^{-1} kanamycin and the culture was incubated at 37 °C with shaking at 200 rpm. When the optical density of the broth at 600 nm reached 0.6–0.8, *Ps*MIaseA was induced by isopropyl β- D-thiogalactopyranoside (IPTG) of 6 mmol L^{-1}, and the culture continued to grow at 16 °C for 12 h.

Purification of the Mannose Isomerase

The culture (200 mL) was centrifugated at 10,000 ×*g* for 5 min. The pellets were mixed with 20 mL of buffer A (20 mmol L^{-1} Tris-HCl, 20 mmol L^{-1} imidazole, 500 mmol L^{-1} NaCl, pH 8.0), and decomposed by ultrasonication for 20 min. After centrifugation (10,000 ×*g*) for 10 min, the supernatant was collected and loaded onto a Ni-NTA column (10 × 50 mm, GE Healthcare) at a flow rate of 0.5 mL min^{-1}. Purification of the mannose isomerase (designated as *Ps*MIaseA) was performed through fast protein liquid chromatography (FPLC, ÄKTA purifier, GE Healthcare), and the system flow rate was set to 1.0 mL min^{-1}. The column was washed successively with six column volumes of buffer A and buffer B (20 mmol L^{-1} Tris-HCl, 50 mmol L^{-1} imidazole, 500 mmol L^{-1} NaCl, pH 8.0) to elute the weak-bonded proteins. Buffer C (20 mmol L^{-1} Tris-HCl, 200 mmol L^{-1} imidazole, 500 mmol L^{-1} NaCl, pH 8.0) was then used to elute the bound proteins. The purity of eluted fractions with mannose isomerase activity was monitored by sodium dodecyl sulfate-polyacrylamide gel electrophoresis (SDS-PAGE). Subsequently, the fractions with high enzyme activity were combined and then dialyzed against 20 mmol L^{-1} Tris-HCl buffer (pH 8.0) at 4 °C overnight. The enzyme was then concentrated using an ultrafiltration tube (nominal molecular mass limit 10,000 Da, BioDee).

Enzyme Assay and Protein Concentration

The mannose isomerase assay was estimated using mannose as the substrate with a fructose assay kit. A mixture containing 0.1 mL diluted enzyme and 0.9 mL mannose liquor (1.0%,

w/v, 50 mmol L^{-1} phosphate, pH 7.5) was reacted at 40 °C for 10 min, and the reaction was terminated by boiling the mixture for 5 min. A total of 50 μL of the above mixture was added to 1.5 mL color-developing agent and boiled for 8 min for coloration. After cooling by rinsing with water, the absorption of the solution at 285 nm was immediately determined. One unit of enzyme activity was defined as the amount of mannose isomerase that liberates 1 μmol of fructose per minute under the conditions described. According to Lowry's method [29], the protein content was measured using bovine serum albumin as standard.

Measurement of Molecular Mass

Two methods, *viz.* SDS-PAGE and gel filtration, were used to measure the molecular masses of *Ps*MIaseA. SDS-PAGE was done in accordance with Laemmli's method using 12.5% separating gel [30]. Coomassie Brilliant Blue R-250 as staining solution was used to make protein bands visible. Gel-filtration was carried out to measure the native molecular mass of *Ps*MIaseA using a Sephacryl-100 column (10 × 400 mm) equilibrated with 20 mmol L^{-1} of phosphate (pH 7.0) containing 150 mmol L^{-1} NaCl. The proteins were eluted by an ÄKTA purifier at a flow rate of 0.5 mL min^{-1}. Phosphorylase b (97.2 kDa), bovine serum albumin (66.5 kDa), ovalbumin (44.3 kDa), α-chymotrypsinogen a (from bovine pancreas, 25.6 kDa), and cytochrome c (12.4 kDa) were used as standards.

Biochemical Characterization of Mannose Isomerase

Optimal pH of *Ps*MIaseA was estimated by standard assay in 50 mmol L^{-1} of different buffers (pH 3.0–11.0) at 40 °C. The buffers used were citrate (pH 3.0–6.0), acetate (pH 4.0–6.0), phosphate (pH 6.0–8.0), tris (hydroxymethyl) aminomethane-HCl (Tris-HCl) (pH 7.0–9.0), 2-(cyclohexylamino) ethanesulfonic acid (CHES) (pH 8.0–10.0), and (cyclohexylamino)-1-propanesulfonic acid (CAPS) (pH 10.0–11.0). After the enzyme was incubated in the above buffers at 30 °C for 30 min, the pH stability was assessed by the residual activity of *Ps*MIaseA.

Optimal temperature of *Ps*MIaseA was evaluated at a temperature range of 10–70 °C in 50 mmol L^{-1} phosphate (pH 7.5). To investigate the thermostability, the residual activity of *Ps*MIaseA was determined after incubation at different temperatures in 50 mmol L^{-1} phosphate (pH 7.5) for 30 min. For the thermal denaturation, *Ps*MIaseA was incubated in 50 mmol L^{-1} phosphate (pH 7.5) at 40, 45, and 50 °C for 8 h, and aliquots were taken at different time intervals to measure their residual activities.

The effects of metal ions and chemical reagents on *Ps*MIaseA were also measured. The enzyme was incubated in 50 mmol L^{-1} phosphate (pH 7.5) with 1 mmol L^{-1} metal ions or chemical reagents at 30 °C for 30 min. Metal ions included Na^{+}, Ag^{+}, K^{+}, Mg^{2+}, Ba^{2+}, Zn^{2+}, Ca^{2+}, Ni^{2+}, Cu^{2+}, Fe^{2+}, Mn^{2+}, Cr^{2+}, Co^{2+}, and Fe^{3+}. Chemical regents included cetyltrimethyl ammonium bromide (CTAB), sodium dodecyl sulfonate (SDS), ethylene diamine tetraacetic acid (EDTA), and β-mercaptoethanol. The residual activities were then determined according to the standard assay. No metal ions or chemical reagents were present in the reaction as the control group. All experiments were carried out in triplicate.

Substrate Specificity and Kinetic Parameters of the Mannose Isomerase

The substrate specificity of *Ps*MIaseA was measured in 50 mmol L^{-1} phosphate (pH 7.5) at 40 °C for 10 min using 1.0% (w/v) of different monosaccharides (mannose, fructose, lyxose,

glucose, D-allulose, D-galactose, D-talose, D-tagatose, D-xylulose, and D-altrose) and disaccharides (mannobiose, lactulose, epilactose, 4-O-β-mannopyranosyl- D-fructofuranose). The sugars produced by isomerization were analyzed by high-performance liquid chromatography (HPLC, Agilent 1260 Infinity II system) with Aminex HPX-87C column (7.8 × 300 mm, Bio-Rad) and refractive index detector (RID, G7162A, Agilent 1260 RID). The column temperature was maintained at 85 °C and the flow rate was 0.6 mL min^{-1}. Monosaccharides and disaccharides mentioned above were used as standards.

Kinetic parameters of *Ps*MIaseA towards mannose and fructose were determined at 40 °C for 5 min. The concentrations of mannose and fructose were selected in the range of 10–100 and 50–400 mmol L^{-1}, respectively. The isomerization products were detected by the HPLC-RID described above. The software GraFit (Erithacus Software, UK) was applied to calculate kinetic parameters (K_m and V_{max}).

Structure Prediction and Molecular Docking Analysis

The 3D structure of *Ps*MIaseA was homology-modeled by the SWISS-MODEL Server (https://swissmodel.expasy.org/) with the crystal structure of *Se*YihS (PDB code 2AFA, 44.6% identity) from *Salmonella enterica* as the template. The mannose and Glcβ1-4Man molecules were docked to *Ps*MIaseA through superimposing with *Se*YihS-mannose (PDB code 2ZBL) and *Rm*CE-Glcβ1-4Man (PDB code 3WKG), respectively. Molecular visualization and graph drawing were conducted using the PyMOL software (version 2.3.1).

Conversion of Fructose for Mannose Production

The total reaction volume of 10 mL consisted of *Ps*MIaseA and fructose dissolved in 50 mmol L^{-1} phosphate (pH 7.5). To optimize the conversion conditions, the effects of different factors such as enzyme dosages (5–70 U mL^{-1}), fructose concentration (400–800 g L^{-1}), and reaction time (0.25–12 h) on mannose production were evaluated step-by-step. The reaction was conducted at 40 °C with a stirring rate of 100 rpm. Samples taken out at different time intervals were boiled for 5 min to deactivate the enzyme. The concentration of mannose was detected by the HPLC-RID, and the space-time yield of mannose was calculated as below:

$$Y_{spt} = c_m / T$$

where Y_{spt} is the space-time yield of mannose (g L^{-1} h^{-1}), c_m is the concentration of mannose in the reaction system (g L^{-1}), and T is the reaction time (h).

Results and Discussion

Cloning and Sequence Analysis of *Ps*MIaseA

A putative gene from *P. syringae* annotated as an N-acylglucosamine 2-epimerase (AGE) family epimerase/isomerase in the GenBank database was cloned into the pET28a (+) vector. The gene with 1245 bp encoded a polypeptide of 414 amino acid residues. BLAST program (http://www.ncbi.nlm.gov/blast) was performed to conduct multiple amino acid sequences alignment between *Ps*MIaseA and other characterized mannose isomerases. *Ps*MIaseA

showed the highest homology of 50.4% with ManI from *T. fusca* (GenBank accession number WP_061783687.1), followed by mannose isomerase from *E. coli* (GenBank accession number AJH12524.1, 44.8%), sulfoquinovose isomerase from *S. enterica* (GenBank accession number Q8ZKT7.1, 44.5%), and Marme_2490 from *Marinomonas mediterranea* (GenBank accession number WP_013661626.1, 30.9%) (Fig. 1). Comparison of the primary sequence of

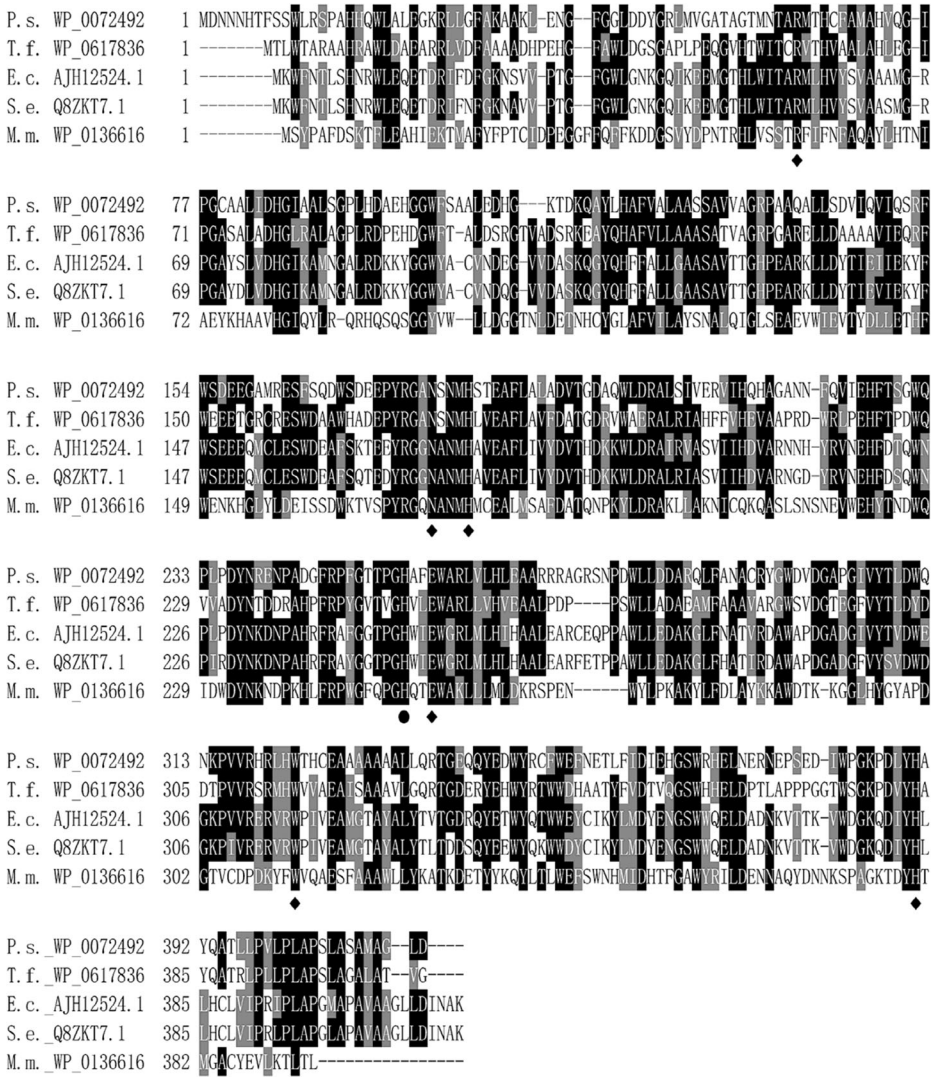

Fig. 1 Multiple alignment of amino acid sequences of *Ps*MIaseA and other mannose isomerases. The residue numbers of the first amino acid in each row are marked on the left. Black shading represents identical residues, while gray shading shows similar residues. Abbreviations and accession numbers of the mannose isomerases are as follows: *Ps*MIaseA from *Pseudomonas syringae* (P.s. WP_007249212.1), ManI from *Thermobifda fusca* (T.f. WP_061783687.1), mannose isomerase from *Escherichia coli* (E.c. AJH12524.1), sulfoquinovose isomerase from *Salmonella enterica* (S.e. Q8ZKT7.1), and Marme_2490 from *Marinomonas mediterranea* (M.m. WP_013661626.1). The conserved catalytic residue (His255) is indicated by a circle, and the residues associated with substrate binding are denoted by diamonds

*Ps*MIaseA with these mannose isomerases indicates that His255 acts as a general base and acid catalyst. Moreover, Arg63, Asn179, His183, Glu258, Trp323, and His390 are related to the substrate binding [21].

Heterologous Expression and Purification of *Ps*MIaseA

The mannose isomerase gene (*PsMIaseA*) was successfully expressed in *E. coli* BL21 with a His_6-tag at the N-terminus. The recombinant enzyme (*Ps*MIaseA) was purified through one step affinity chromatography with 75% recovery yield and 1.3-fold purification. A single homogenous band was shown on SDS-PAGE with a molecular mass around 44.0 kDa (Fig. 2), which is accordance with the predicted molecular mass of 46.1 kDa. This is similar to many other mannose isomerases with molecular masses ranging from 42.0 to 51.4 kDa, such as Marme_2490 from *M. mediterranea* NBRC 103028 [21] and *Se*YihS from *S. enterica* [23]. The apparent molecular mass of *Ps*MIaseA was further measured by Sephacryl-100 gel filtration chromatography to be 40.5 kDa, indicating that *Ps*MIaseA is a monomer. This is different from the mannose isomerases from *Agrobacterium radiobacter* M-1 and *E. coli* BL21, which exist as dimer and hexamer, respectively [25, 27].

Biochemical Characterization of *Ps*MIaseA

*Ps*MIaseA showed the maximum activity at pH 7.5 (Fig. 3a). The enzyme was stable in the pH range of 5.0–10.0, where it maintained more than 80% of the maximum activity (Fig. 3b). The purified *Ps*MIaseA displayed the highest activity at 40 °C and showed 40% activity at 10 °C (Fig. 3c). *Ps*MIaseA was thermostable up to 45 °C, exhibiting more than 80% of the maximum activity (Fig. 3d). The half-lives of *Ps*MIaseA at 40, 45, and 50 °C were 543.2, 345.0, and 29.2 min, respectively (Fig. 3e). The impact of some metal ions and reagents on *Ps*MIaseA was further determined (Table 1). *Ps*MIaseA was strongly inhibited by Ag^+ (36.6%), Cu^{2+} (34.1%), and CTAB (40.8%). However, other metal ions and reagents showed no remarkable effects on the mannose isomerase.

The pH optimum of *Ps*MIaseA is quite different from the mannose isomerase from *P. cepacian* having weakly acid optimal pH (6.2) [31]. It is similar to the optimal pH values of most other mannose isomerases, which are in weakly alkaline mediums around pH 7.5–8.0, such as those from *A. radiobacter* M-1 (pH 8.0) [27], *P. saccharophila* (pH 7.5) [20], and *X. rubrilineans* S-48 (pH 7.8) [22]. The optimal temperature of *Ps*MIaseA is higher than that of Marme_2490 from *M. mediterranea* NBRC 103028 (30 °C) [21] and is much lower than those of the enzymes from *A. radiobacter* M-1 (60 °C) [27] and *T. fusca* MBL10003 (60 °C) [24]. Although high reaction temperature can reduce microbial contamination and increase reaction rate [32], it also significantly enhances the rate of Maillard reaction and chemical conversion [33]. Thus, the low optimal temperature of *Ps*MIaseA is beneficial for avoiding the by-products (melanin and glucose). Moreover, most metal ions and EDTA did not affect the activity of *Ps*MIaseA, suggesting that the isomerization of this enzyme does not depend on metal ions. The lyxose isomerase, another enzyme that can be used to produce mannose, is a metal-dependent enzyme [18], which means that metal ions must be removed from the reaction system after isomerization. Therefore, *Ps*MIaseA could catalyze the isomerization at mild condition without metal ion dependent, which are the advantages of this enzyme for the green production of mannose.

Substrate Specificity and Kinetic Parameters

*Ps*MIaseA showed high specific activity towards mannose and fructose, which were 818.6 and 273.8 U mg^{-1}, respectively. The enzyme had no detectable activity towards other monosaccharides and disaccharides (Table S1). Then, the kinetic parameters of *Ps*MIaseA were investigated using mannose and fructose as substrates (Table 2). Kinetic parameters of *Ps*MIaseA for mannose were 36.6 mmol L^{-1} of K_m and 1044.6 μmol min^{-1} mg^{-1} of V_{max}, while those for fructose were 175.5 mmol L^{-1} of K_m and 792.6 μmol min^{-1} mg^{-1} of V_{max}.

The specific activity of *Ps*MIaseA towards mannose is much higher than that of the mannose isomerases from *A. radiobacter* M-1 (231 U mg^{-1}) [27], *P. cepacia* (126 U mg^{-1}) [31], and *T. fusca* MBL10003 (69.2 U mg^{-1}) [24]. *Ps*MIaseA showed strict substrate specificity, which only catalyzed the isomerization between mannose and fructose. In contrast, the mannose isomerase from *T. fusca* MBL10003 can isomerize mannose and lyxose [24], whereas Marme_2490 from *M. mediterranea* NBRC 103028 displays wide substrate specificity for different monosaccharides and disaccharides [21]. The 3D structure of *Ps*MIaseA was further homology-modeled with *Se*YihS (PDB code 2AFA) as template. The overall structure of *Ps*MIaseA contained a typical $(\alpha/\alpha)_6$-barrel domain and a deep slot-like pocket which can bind one mannose molecule (Fig. S1a). Six substrate binding residues (Arg63, Asn179, His183, Glu258, Trp323, and His390) and the catalytic residue (His255) surrounded the mannose (Fig. S1b). In *Se*YihS, the α7-α8 and α11-α12 loops show good flexibility and are distal from the substrate-binding site in the mannose-free form [23]. After binding

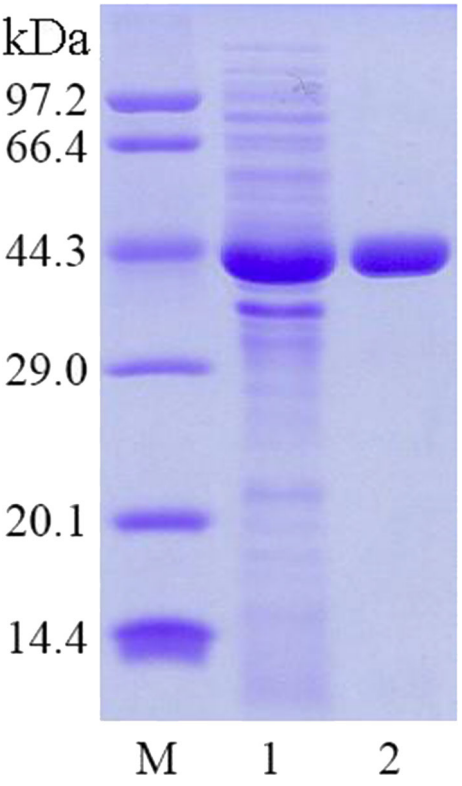

Fig. 2 SDS-PAGE of the purified *Ps*MIaseA. Lanes represent low-molecular mass protein standards (lane M), crude lysate (lane 1), and purified *Ps*MIaseA (lane 2), respectively

mannose, the Phe239 in α7-α8 loop and the Trp375 in α11-α12 loop form hydrophobic interaction with the 4-C, 5-C, and 6-C of mannose. The two loops are situated near the mannose and close the substrate-binding site entrance of *Se*YihS (Fig. S1c). Similar to *Se*YihS, Phe246 and Trp382 were located in the α7-α8 and α11-α12 loops of *Ps*MIaseA, respectively, corresponding to Phe239 and Trp375 of *Se*YihS. The two loops of *Ps*MIaseA presumably covered the catalytic pocket after binding the mannose molecule (Fig. S1d). Phe246 and

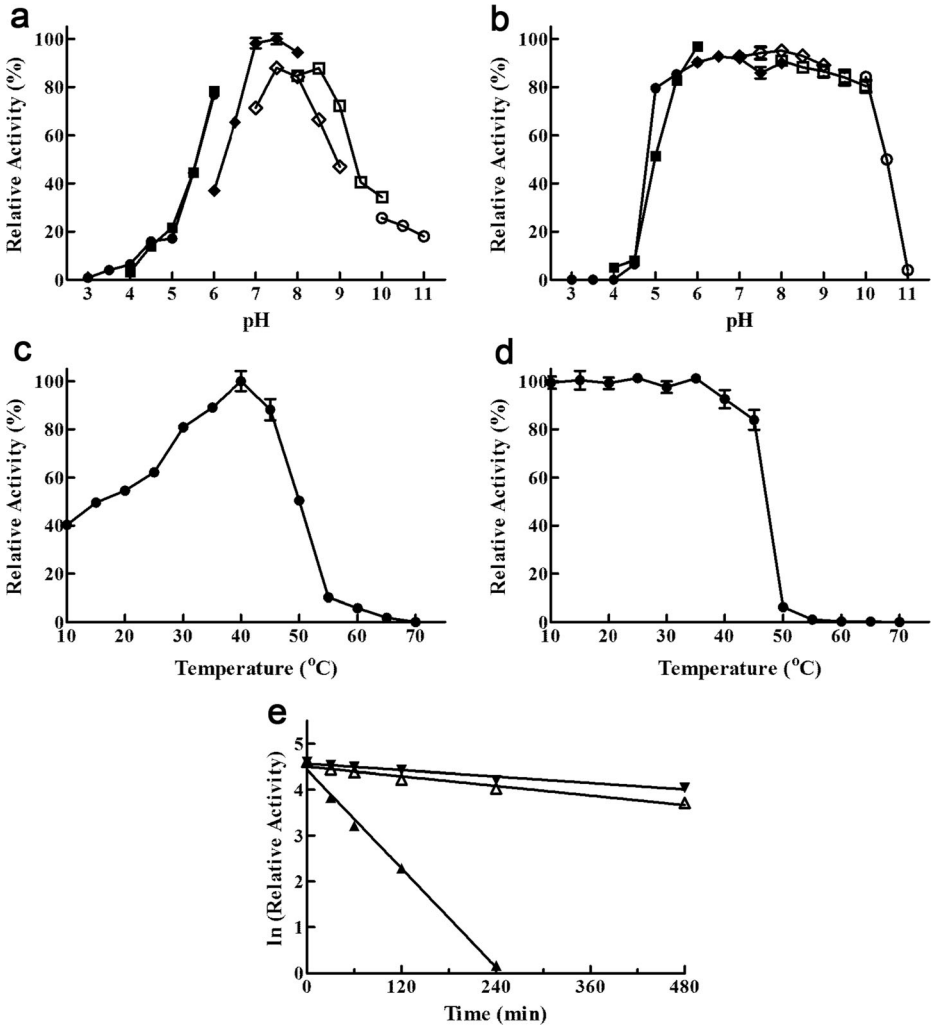

Fig. 3 Optimal pH (**a**), pH stability (**b**), optimal temperature (**c**), thermostability (**d**), and thermal denaturation (**e**) of purified *Ps*MIaseA. To measure the optimal pH of *Ps*MIaseA, the reaction was performed in different buffers (50 mmol L^{-1}) at 40 °C for 10 min. The evaluation of pH stability was performed by incubating the enzyme in different buffers at 30 °C for 30 min, and the residual activity was determined by standard assay. Citrate (●), acetate (■), phosphate (◆), Tris-HCl (◇), CHES (□), and CAPS (○) were buffers used. To determine the optimal temperature, the reaction was carried out at different temperatures in phosphate buffer (50 mmol L^{-1}, pH 7.5) for 10 min. For thermostability, the residual activity was tested after incubation at different temperatures for 30 min. For thermal denaturation, *Ps*MIaseA was incubated at 40 (▼), 45 (△), and 50 (▲) °C for 8 h, and the residual activity was estimated by standard assay

Table 1 Effect of different metal ions and chemical reagents on the activity of purified *Ps*MIaseA

Metal ions and chemical reagents	Specific activity (U mg^{-1})	Relative activity (%)
control	818.6 ± 2.3	100
Na^{+}	764.6 ± 2.2	93.4
K^{+}	682.7 ± 0.9	83.4
Ag^{+}	299.6 ± 3.1	36.6
Mg^{2+}	719.5 ± 3.7	87.9
Ca^{2+}	830.9 ± 4.3	101.5
Ba^{2+}	753.9 ± 2.8	92.1
Zn^{2+}	749.0 ± 0.9	91.5
Ni^{2+}	748.2 ± 1.1	91.4
Mn^{2+}	777.7 ± 4.1	95.0
Cu^{2+}	279.1 ± 1.9	34.1
Fe^{2+}	821.1 ± 1.8	100.3
Cr^{2+}	745.7 ± 2.1	91.1
Co^{2+}	738.4 ± 3.4	90.2
Fe^{3+}	776.0 ± 1.5	94.8
CTAB	334.0 ± 3.1	40.8
EDTA	751.5 ± 2.3	91.8
SDS	684.3 ± 4.5	83.6
β-Mercaptoethanol	804.7 ± 1.9	98.3

The enzyme was incubated at 30 °C for 30 min with 1 mmol L^{-1} different metal ions and chemical reagents, and the residual activities were determined. Values represent the mean ± SD (n = 3) with respect to the untreated control samples

Trp382 are predicted to cause severe steric hindrance to prevent disaccharide substrate from entering the catalytic pocket in both *Se*YihS and *Ps*MIaseA (Fig. S1e). Therefore, *Ps*MIaseA showed strict substrate specificity towards mannose and fructose. However, in Marme_2490 (PDB code 5X32), a mannose isomerase which can catalyze disaccharide, the α7-α8 loop is ordered and the α11-α12 loop is in close proximity to α2, suggesting that Marme_2490 has an open substrate-binding site to accommodate and catalyze disaccharide substrates (Fig. S1f) [21]. Similar structure can be observed in a cellobiose 2-epimerase from *Rhodothermus marinus* (*Rm*CE) [34]. The high catalytic efficiency and strict substrate specificity make the enzyme a good candidate for mannose production.

Mannose Production by *Ps*MIaseA

Different dosage of *Ps*MIaseA (5–70 U mL^{-1}) was evaluated in 500 g L^{-1} fructose at 40 °C for 8 h. The yield of mannose was gradually improved with the increase of *Ps*MIaseA dosage, and was up to 137 g L^{-1} when 20 U mL^{-1} of *Ps*MIaseA was used (Fig. 4a). Fructose concentrations ranging from 400 to 800 g L^{-1} were then used for mannose production. The yield of mannose was 163 g L^{-1} in 600 g L^{-1} fructose (Fig. 4b). Although mannose yield was 176 g L^{-1} in 800 g

Table 2 Kinetic parameters of *Ps*MIaseA for mannose and fructose (mean ± SD)

Substrate	V_{max} (μmol min^{-1} mg^{-1})	K_m (mmol L^{-1})	k_{cat} (s^{-1})	k_{cat}/K_m (L s^{-1} $mmol^{-1}$)
Mannose	1044.6 ± 20.2	36.6 ± 2.2	0.766	0.021
Fructose	792.6 ± 19.5	175.5 ± 10.1	0.581	0.003

Enzyme reactions were performed in phosphate buffer (50 mmol L^{-1}, pH 7.5) at 40 °C for 5 min with mannose or fructose as a substrate

L^{-1} fructose, high fructose concentration (650–800 g L^{-1}) resulted in obvious conversion reduction. Furthermore, the reaction time of mannose production was investigated. Basically, mannose yield was enhanced and fructose concentration was reduced with the reaction time (Fig. 4c). The reaction was almost in equilibrium at 6 h, with a fructose conversion rate of 27%

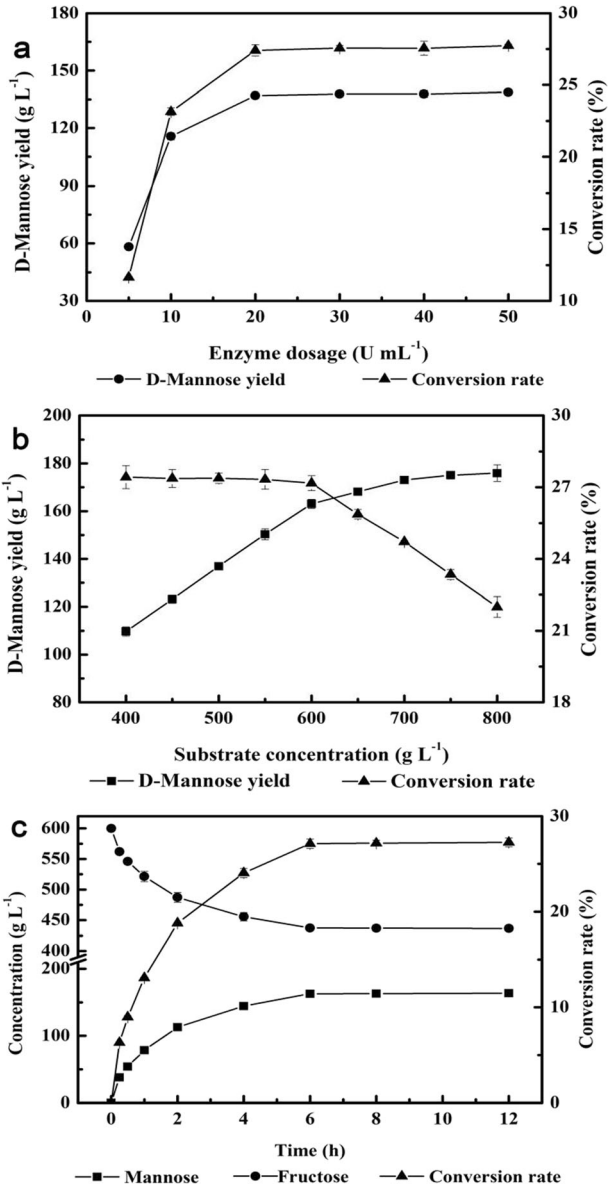

Fig. 4 Optimization of mannose production by *Ps*MIaseA. **a** The effect of enzyme dosage on mannose production. Different dosage (5–70 U mL^{-1}) of *Ps*MIaseA was mixed with 500 g L^{-1} fructose, and the reaction was performed at 40 °C for 8 h. **b** The influence of substrate concentration on mannose production. *Ps*MIaseA (20 U mL^{-1}) was mixed with different concentrations of fructose (400 to 800 g L^{-1}), and the reaction was conducted at 40 °C for 8 h. **c** Time course of mannose production by *Ps*MIaseA. The enzyme (20 U mL^{-1}) was mixed with 600 g L^{-1} fructose, and the reaction was performed at 40 °C for 12 h

and a mannose yield of 163 g L^{-1}. The space-time yield of mannose was 27.2 g L^{-1} h^{-1} after 6 h reaction.

To achieve an economical mannose production process, it is necessary to minimize the enzyme dosage. Although high substrate concentration can improve the production yield, high concentration leads to high viscosity and low fluidity of reaction system, causing a low efficiency of the production [35]. Thus, enzyme dosage and fructose concentration were optimized. A dose of 20 U mL^{-1} of *Ps*MIaseA and a fructose concentration of 600 g L^{-1} were selected for mannose production. After 6 h reaction, the fructose conversion rate was 27%, which is comparable with those of the mannose isomerases from *M. mediterranea* NBRC 103028 (30%) [21], *T. fusca* MBL10003 (25%) [24], and *E. coli* BL21 (25%) [25]. Furthermore, the space-time yield of mannose was 27.2 g mannose L^{-1} h^{-1}. This yield is much higher than that of other enzymes for mannose production, such as the lyxose isomerase from *Caldanaerobius polysaccharolyticus* (6.4 g mannose L^{-1} h^{-1}) [36], the lyxose isomerase from *Thermoflavimicrobium dichotomicum* (18.4 g mannose L^{-1} h^{-1}) [18], and the mannose 2-epimerase from *Runella slithyformis* (2.5 g mannose L^{-1} h^{-1}) [37]. Thus, *Ps*MIaseA showing high production efficiency may be beneficial for the green production of mannose.

Conclusion

A novel mannose isomerase (*Ps*MIaseA) from *P. syringae* was successfully expressed in *E. coli*. *Ps*MIaseA showed high specific activity and catalytic efficiency at a moderate temperature and pH condition. The enzyme could convert fructose for mannose production with a high conversion rate of 27%. At the optimal condition, the space-time yield of mannose was up to 27.2 g L^{-1} h^{-1} with a high productivity for mannose. Therefore, *Ps*MIaseA may be a potential candidate for mannose production.

Supplementary Information The online version contains supplementary material available at https://doi.org/10.1007/s12010-021-03487-y.

Authors' Contributions Conceptualization, methodology, data curation, investigation, and writing—original draft preparation: Xiaohan Hua and Yanxiao Li. Conceptualization, methodology, and investigation: Junwen Ma. Conceptualization, supervision, and writing—review and editing: Zhengqiang Jiang. Supervision: Haijie Liu. Supervision and writing—review and editing: Qiaojuan Yan. All the authors read and approved the final manuscript.

Funding This work was supported by the National Natural Science Foundation of China (No. 31901627), and the key state research and development plan "Modern Food Processing and Food Storage and Transportation Technology and Equipment" (No. 2016YFD0400804).

Compliance with Ethical Standards

Conflict of Interest The authors declare that they have no conflict of interest.

Ethical Approval Not applicable.

Consent to Participate Not applicable.

Consent to Publish Not applicable.

References

1. Huang, J. W., Yu, L. N., Zhang, W. L., Zhang, T., Guang, C., & Mu, W. M. (2018). Production of D-mannose from D-glucose by co-expression of D-glucose isomerase and D-lyxose isomerase in *Escherichia coli*. *Journal of the Science of Food and Agriculture, 98*(13), 4895–4902.
2. Pohl, J. B., Baldwin, B. A., Dinh, B. L., Rahman, P., Smerek, D., Prado, F. J., Sherazee, N., & Atkinson, N. S. (2012). Ethanol preference in *Drosophila melanogaster* is driven by its caloric value. *Alcoholism: Clinical & Experimental Research, 36*(11), 1903–1912.
3. Ghlissi, Z., Kallel, R., Krichen, F., Hakim, A., Zeghal, K., Boudawara, T., Bougatef, A., & Sahnoun, Z. (2019). Polysaccharide from *Pimpinella anisum* seeds: structural characterization, anti-inflammatory and laser burn wound healing in mice. *International Journal of Biological Macromolecules, 156*, 1530–1538.
4. Kranjčec, B., Papeš, D., & Altarac, S. (2014). D-Mannose powder for prophylaxis of recurrent urinary tract infections in women: a randomized clinical trial. *World Journal of Urology, 32*(1), 79–84.
5. Sanders, M. E., Merenstein, D. J., Reid, G., Gibson, G. R., & Rastall, R. A. (2019). Probiotics and prebiotics in intestinal health and disease: from biology to the clinic. *Nature Reviews Gastroenterology & Hepatology, 16*(10), 605–616.
6. Gonzalez, P. S., O'Prey, J., Cardaci, S., Barthet, V. J., Sakamaki, J. I., Beaumatin, F., Roseweir, A., Gay, D. M., Mackay, G., & Malviya, G. (2018). Mannose impairs tumour growth and enhances chemotherapy. *Nature, 563*(7733), 719–723.
7. Berge, A. C., & Wierup, M. (2012). Nutritional strategies to combat Salmonella in mono-gastric food animal production. *Animal, 6*(4), 557–564.
8. Chen, F. E., Zhao, J. F., Xiong, F. J., Xie, B., & Zhang, P. (2007). An improved synthesis of a key intermediate for (+)-biotin from D-mannose. *Carbohydrate Research, 342*(16), 2461–2464.
9. Saloranta, T., Peuronen, A., Dieterich, J. M., Ruokolainen, J., Lahtinen, M., & Leino, R. (2016). From mannose to small amphiphilic polyol: perfect linearity leads to spontaneous aggregation. *Crystal Growth & Design, 16*(2), 655–661.
10. Wei, Z. W., Huang, L. F., Cui, L., & Zhu, X. (2020). Mannose: good player and assister in pharmacotherapy. *Biomedicine & Pharmacotherapy, 129*, 110420.
11. Shintani, T. (2019). Food industrial production of monosaccharides using microbial, enzymatic, and chemical methods. *Fermentation, 5*(2), 47–59.
12. Monteiro, A. F., Miguez, I. S., Silva, J. P. R. B., & da Silva, A. S. (2019). High concentration and yield production of D-mannose from açaí (*Euterpe oleracea* Mart.) seeds via mannanase-catalyzed hydrolysis. *Scientific Reports, 9*(1), 10939–10950.
13. Mussatto, S. I., Carneiro, L. M., Silva, J. P. A., Roberto, I. C., & Teixeira, J. A. (2011). A study on chemical constituents and sugars extraction from spent coffee grounds. *Carbohydrate Polymers, 83*(2), 368–374.
14. Hu, H., Liu, S. R., Zhang, W. Z., An, J. H., & Xia, H. A. (2020). Efficient epimerization of glucose to mannose over molybdenum-based catalyst in aqueous media. *Chemistry Select, 5*(5), 1728–1733.
15. Hu, X., Shi, Y. N., Zhang, P., Miao, M., Zhang, T., & Jiang, B. (2016). D-Mannose: properties, production, and applications: an overview. *Comprehensive Reviews in Food Science and Food Safety, 15*(4), 773–785.
16. Wu, H., Zhang, W., & Mu, W. (2019). Recent studies on the biological production of D-mannose. *Applied Microbiology and Biotechnology, 103*(21-22), 8753–8761.
17. Park, C. S., Kim, J. E., Choi, J. G., & Oh, D. K. (2011). Characterization of a recombinant cellobiose 2-epimerase from *Caldicellulosiruptor saccharolyticus* and its application in the production of mannose from glucose. *Applied Microbiology and Biotechnology, 92*(6), 1187–1196.
18. Zhang, W. L., Huang, J. W., Jia, M., Guang, C., Zhang, T., & Mu, W. M. (2019). Characterization of a novel D-lyxose isomerase from *Thermoflavimicrobium dichotomicum* and its application for D-mannose production. *Process Biochemistry, 83*, 131–136.
19. Hirose, J., Kinoshita, Y., Fukuyama, S., Hayashi, S., Yokoi, H., & Takasaki, Y. (2003). Continuous isomerization of D-fructose to D-mannose by immobilized *Agrobacterium radiobacter* cells. *Biotechnology Letters, 25*(4), 349–352.
20. Palleroni, N. J., & Doudoroff, M. (1956). Mannose isomerase of *Pseudomonas saccharophila*. *Journal of Biological Chemistry, 218*(1), 535–548.
21. Saburi, W., Jaito, N., Kato, K., Tanaka, Y., Yao, M., & Mori, H. (2018). Biochemical and structural characterization of *Marinomonas mediterranea* D-mannose isomerase Marme_2490 phylogenetically distant from known enzymes. *Biochimie, 114*, 63–73.
22. Takasaki, Y., Takano, S., & Tanabe, O. (1964). Studies on the isomerization of sugars by bacteria. VIII. Purification and some properties of D-mannose isomerase from *Xanthomonas rubrilineans* S-48. *Agricultural and Biological Chemistry, 28*(9), 605–609.

23. Itoh, T., Mikami, B., Hashimoto, W., & Murata, K. (2008). Crystal Structure of YihS in Complex with D-mannose: structural annotation of *Escherichia coli* and *Salmonella enterica yihS*-encoded proteins to an aldose-ketose isomerase. *Journal of Molecular Biology, 377*(5), 1443–1459.
24. Kasumi, T., Mori, S., Kaneko, S., Matsumoto, H., Kobayashi, Y., & Koyama, Y. (2014). Characterization of mannose isomerase from a cellulolytic actinobacteria *Thermobifida fusca* MBL10003. *Journal of Applied Glycoscience, 61*(1), 21–25.
25. Hu, X., Zhang, P., Miao, M., Zhang, T., & Jiang, B. (2016). Development of a recombinant D-mannose isomerase and its characterizations for D-mannose synthesis. *International Journal of Biological Macromolecules, 89*, 328–335.
26. Hey-Ferguson, A., & Elbein, A. D. (1970). Purification of a D-mannose isomerase from *Mycobacterium smegmatis*. *Journal of Bacteriology, 101*(3), 777–780.
27. Hirose, J., Maeda, K., Yokoi, H., & Takasaki, Y. (2001). Purification and characterization of mannose isomerase from *Agrobacterium radiobacter* M-1. *Bioscience, Biotechnology, and Biochemistry, 65*(3), 658–661.
28. Xin, X. F., Kvitko, B., & He, S. Y. (2018). *Pseudomonas syringae*: what it takes to be a pathogen. *Nature Reviews Microbiology, 16*(5), 316–328.
29. Lowry, O. H., Rosebrough, N. J., Farr, A. L., & Randall, R. J. (1951). Protein measurement with the Folin phenol reagent. *Journal of Biological Chemistry, 193*(1), 265–275.
30. Laemmli, U. K. (1970). Cleavage of structural proteins during assembly of head of bacteriophage T4. *Nature, 227*(5258), 680–685.
31. Allenza, P., Morrell, M. J., & Detroy, R. W. (1990). Conversion of mannose to fructose by immobilized mannose isomerase from *Pseudomonas cepacian*. *Applied Biochemistry and Biotechnology, 24*, 171–182.
32. Mozhaev, V. V. (1993). Mechanism-based strategies for protein thermostabilization. *Trends in Biotechnology, 11*(3), 88–95.
33. Shen, S. C., & Wu, J. S. B. (2004). Maillard browning in ethanolic solution. *Journal of Food Science, 69*(4), 273–279.
34. Fujiwara, T., Saburi, W., Matsui, H., Mori, H., & Yao, M. (2014). Structural insights into the epimerization of β-1,4-linked oligosaccharides catalyzed by cellobiose 2-epimerase, the sole enzyme epimerizing non-anomeric hydroxyl groups of unmodified sugars. *Journal of Biological Chemistry, 289*(6), 3405–3415.
35. Geng, W., Jin, Y., Jameel, H., & Park, S. (2015). Strategies to achieve high-solids enzymatic hydrolysis of dilute-acid pretreated corn stover. *Bioresource Technology, 187*, 43–48.
36. Wu, H., Chen, M., Guang, C. E., Zhang, W. L., & Mu, W. M. (2020). Characterization of a recombinant D-mannose-producing D-lyxose isomerase from *Caldanaerobius polysaccharolyticus*. *Enzyme and Microbial Technology, 138*, 109553.
37. Saburi, W., Sato, S., Hashiguchi, S., Muto, H., Iizuka, T., & Mori, H. (2019). Enzymatic characteristics of D-mannose 2-epimerase, a new member of the acylglucosamine 2-epimerase superfamily. *Applied Microbiology and Biotechnology, 103*(16), 6559–6570.